THE ASTROPHYSICAL JOURNAL, 346:201–211, 1989 November 1

CO IN PLANETARY NEBULAE

P. J. HUGGINS AND A. P. HEALY
Physics Department, New York University
Received 1989 February 21; accepted 1989 April 29

ABSTRACT

A survey has been carried out in the CO(2–1) line to search for molecular gas in 100 planetary nebulae. Nineteen show evidence of CO emission, a few of which were known from earlier studies. The detected nebulae are mainly younger disk population objects formed from high-mass progenitors according to their morphological types and nitrogen-to-oxygen ratios. Rough estimates show a large range in the masses of the molecular envelopes from about 1 $M_\odot$ to less than 10^{-3} $M_\odot$. For the extreme class of objects detected in CO, the ratio of molecular to ionized mass decreases with increasing radius, as expected if the nebulae grow by the ionization of previously ejected molecular envelopes. The molecular gas is the dominant observed mass component in these nebulae, at least until they expand to radii larger than about 0.1 pc, where the bulk of the CO will be dissociated. The absence of substantial CO envelopes in other nebulae may be due to lower mass-loss rates and less effective CO shielding, as well as the longer time scale for the luminosity evolution of low-mass central stars.

Subject headings: nebulae: abundances — nebulae: planetary — radio sources: lines

I. INTRODUCTION

This paper presents the results of a survey in the 230 GHz CO(2–1) line to study molecular gas in planetary nebulae (PNe). It is widely believed that PNe form on a rapid time scale from highly evolved red giant stars, and it is well established that these stars undergo intense mass loss, forming dense circumstellar envelopes of molecular gas. The presence of residual molecular gas in PNe should therefore be important for understanding the formation and subsequent evolution of the nebulae.

Although CO was the first molecule detected in a PN (Mufson, Lyon, and Marionni 1975), further CO searches have turned up few new objects, as summarized by Knapp (1987). As an alternative probe, the near-infrared lines of H_2 have been more useful in demonstrating the presence of molecules in a number of PNe (Webster *et al.* 1988, and references therein). The H_2 observations, however, provide very limited information on the total mass of molecular gas because of the high energy levels and uncertain excitation of the transitions involved. A third molecular species, OH, has also been surveyed and detected in a few PNe (Payne, Phillips, and Terzian 1988, and references therein). Taken together, these observations indicate that molecular gas is an important component of at least some PNe, but the available data are insufficient to provide a quantitative picture.

The present survey was undertaken to reexamine the question of CO in PNe because it is potentially the single most useful probe of the kinematics, distribution, and mass of the molecular gas, as it is in the circumstellar envelopes of red giants. The first results of this work on three PNe of special interest (NGC 7293, NGC 6720, and NGC 2346) were reported earlier (Huggins and Healy 1986*a*, *b* and Healy and Huggins 1988; hereafter Papers 1–3, respectively). In this paper we present more complete results of the survey which includes 100 PNe. Several new detections are reported, and the results of the survey are discussed in the context of the role of molecular gas in the evolution of PNe.

II. OBSERVATIONS AND RESULTS

The observations were made with the NRAO[1] 12 m telescope at Kitt Peak in five observing sessions between 1985 December and 1988 January. The CO(2–1) line was used in preference to the 1–0 line because of the greater sensitivity to small-scale, optically thin emission expected from most PNe. The 200–270 GHz dual channel mixer receiver was used, in most cases with 1 MHz filters, giving a velocity resolution of 1.3 km s^{-1}. The measured beam size of the telescope was 30″–32″.

The data were taken either by position switching the telescope, typically 10′ in azimuth, or by using a nutating secondary with a beam throw of 4′ or 6′; this latter method was used on the smaller sources when the facility became available because of improved baseline subtraction. We made particular efforts to characterize the pointing corrections as well as possible during each observing session. Based on repeated observations of reference sources we estimate that the pointing is good to about 6″ for most of our data on objects which transit to the south at Kitt Peak. For objects which transit to the north there are few strong reference sources and the pointing is worse, possibly 10″ or more in certain regions. This is probably not critical for extended PNe, but could affect the results for compact objects.

The data were calibrated with the chopper wheel technique and further corrected for the effects of the atmosphere on the basis of sky tips. The final data are reported here in terms of the main beam brightness temperature, using efficiencies measured by NRAO. They are thus corrected for forward spillover and error pattern losses.

The 100 PNe observed in the survey are listed in Tables 1 and 2. The emphasis in selecting the sample has been to include objects with a broad range of properties. The sample thus contains different morphological and abundance types, and

[1] The National Radio Astronomy Observatory is operated by Associated Universities, Inc., under contract with the National Science Foundation.

TABLE 1

SURVEY NEBULAE NOT DETECTED

PN[a]	rms[b] (mK)	I[c] (K km s^{-1})	M_m[d] ($M_\odot$)	PN[a]	rms[b] (mK)	I[c] (K km s^{-1})	M_m[d] ($M_\odot$)
NGC 40	65	1.72	1.6(−3)	NGC 6058[f]	66	1.64	2.8(−2)
Vy 1-1	74	1.22	6.3(−3)	IC 4593	81	1.38	6.7(−3)
Hu 1-1	81	1.55	2.6(−2)	NGC 6210	40	0.85	1.2(−3)
NGC 246, 67 W, 65 S	62[e]	1.88	9.4(−3)	NGC 6369	200	4.41[i]	3.6(−2)
M1-1	64	1.12	4.6(−2)	Hb 4	220	5.15	9.2(−3)
NGC 650[f] 20 W, 20 S	110[e]	3.32	1.2(−2)	M1-26[f]	360	...[h]	...
IC 1747	66	1.61	6.7(−3)	NGC 6543	41	0.85	3.1(−4)
M1-2	67	1.33	...[g]	NGC 6572	160	3.12	4.7(−4)
IC 289	270	...[h]	...	NGC 6629	160	1.97	4.5(−3)
M1-4	64	0.93	4.4(−3)	M3-27	66	1.15	...[g]
IC 2003	77	1.70	2.1(−2)	Sh 2-71	200	...[h]	...
NGC 1501[f]	150	4.38	4.3(−2)	NGC 6741	110	2.61	4.3(−3)
NGC 1535	69	1.47	9.6(−3)	M1-67	110	2.38	2.0(−2)
H3-29	82	1.81	...[g]	NGC 6778	120	2.65	3.6(−3)
IC 418	65	1.13	1.0(−4)	NGC 6790	180	3.44[i]	3.4(−3)
H3-75[f]	65	1.43	...[g]	Vy 2-2	43	0.85	1.5(−2)
NGC 2022	140	3.62	2.0(−2)	BD +30°3639	71	1.65	9.3(−4)
M1-5[f]	87	1.02[i]	4.9(−3)	NGC 6826	87	1.37	3.5(−3)
IC 2149	65	1.08	1.5(−3)	NGC 6833	140	1.74	...[g]
A13[f] 45 W, 45 N	250	5.74	7.2(−2)	NGC 6853	97[e]	...[j]	...
IC 2165	200	4.41	3.4(−2)	NGC 6884	110	2.57	5.8(−3)
J900	58	1.22	3.5(−3)	NGC 6881[f]	130	2.48[i]	7.1(−3)
M1-6[f]	67	1.45[i]	...[g]	NGC 6886	148	2.95	5.9(−3)
M3-1	75	1.65	2.8(−2)	NGC 6894	170	5.43	3.5(−2)
M1-9[f]	63	0.69	...[g]	IC 4997	110	2.01	1.9(−2)
NGC 2371	48	1.55	1.3(−2)	M3-35	110	1.82	...[g]
M3-3[f]	91	1.42	7.2(−3)	NGC 7008	78[e]	2.45	1.9(−2)
NGC 2392	57	2.05	4.3(−3)	NGC 7009	83	1.80	2.7(−3)
A21 115 E, 194 N	90[e]	2.43	1.6(−2)	NGC 7026	55	...[h]	...
M1-15[f]	78	1.69[i]	...[g]	NGC 7048	96	1.91[i]	3.1(−2)
NGC 2438	89	2.08	2.2(−2)	K3-62	110	2.57[i]	...[g]
M1-18	74	1.29	1.4(−2)	Hu 1-2	58	1.41[i]	1.1(−2)
NGC 2452	140	3.09	4.8(−2)	NGC 7094	83[e]	2.69	4.5(−2)
A24 80 E, 80 N	60[e]	1.10	5.3(−3)	IC 5217	73	1.14	1.2(−3)
A30[f]	47	1.45	3.1(−2)	Me2-2[f]	110	1.21	...[g]
NGC 2818[f]	62	1.37	2.7(−2)	NGC 7354	99	2.41	6.6(−3)
NGC 3242	59	1.38	1.3(−3)	NGC 7662	110	2.57	2.7(−3)
NGC 3587 13 E, 61 N	95	2.54	1.1(−2)	Hb 12	62	1.05[i]	6.7(−3)
NGC 4361	30	0.91	1.6(−1)	M2-55	82	2.60	2.5(−2)
IC 3568	63	0.89	5.3(−3)	Jn 1[f]	130	2.48	3.4(−2)
IC 972	54	1.07	3.4(−2)				

[a] For observations made off-center the offsets are given in arcseconds.

[b] In a few cases where 2 MHz filters were used the equivalent 1 MHz values are given.

[c] Upper limit on the integrated CO intensity (see text).

[d] Derived limit on the molecular mass (see text).

[e] Other representative positions also observed to about the same limit.

[f] Position references. NGC 650 (Higgs 1969); NGC 1501 (Pottasch 1984); H3-75, M1-15, NGC 2818 (Milne 1973); M1-5, M1-9, M1-26 (Kwok 1985); A 13, M3-3, A30, NGC 6058, Jn 1 (Kaler 1983); M1-6 (Milne 1976); NGC 6881, Me 2-2 (Isaacman 1984*a*).

[g] Distance uncertain.

[h] Strong Galactic line contamination.

[i] Narrow lines present assumed to be Galactic.

[j] See text.

compact as well as highly evolved PNe. It also includes many of the optically bright, nearby PNe which are well studied at other wavelengths. Most of the PNe are within about 3 kpc of the Sun since only very massive molecular envelopes could be expected to be detected at much larger distances.

The coordinates adopted for the centers of the PNe were taken mainly from the catalog of Acker *et al.* (1982). Additional position references are given in footnotes to Tables 1 and 2 for PNe not in the catalog, and for those where improved coordinates differ significantly from the catalog entries. Most PNe were observed only toward the central position, although several with angular sizes larger than the telescope beam were observed at one or more offset positions according to their appearance in optical photographs. We note that the observations can be affected by a patchy CO distribution in large PNe (e.g., Paper 1), limitations in the telescope pointing, and uncertainties in the adopted coordinates, which may occasionally exceed half the beam width even when the nominal uncertainty is much smaller (e.g., Isaacman 1984*a*). A few PNe may prove to have CO emission above the values or limits discussed below, but it is unlikely that our overall conclusions are substantially affected by this.

Of the 100 PNe observed in the survey, CO was not detected in 81. Table 1 lists the rms noise levels of the spectra and upper limits on the CO emission. The limits are 3 σ estimates for the velocity integrated intensities (I) based on the noise levels of the spectra, assuming flat baselines and a velocity width of twice the optical expansion velocity (Sabbadin 1984); if the expansion velocity is not known 20 km s^{-1} is used. For uniformity, these limits are used whether or not the radial velocity of the PN is accurately known. Narrow lines are usually assumed to be Galactic and are ignored, but no limits are given where the

TABLE 2

SURVEY NEBULAE DETECTED IN CO

PN	rms (mK)	T (K)	V_0 (km s^{-1})	V_e (km s^{-1})	I (K km s^{-1})	Notes
AFGL 618	150	2.2	−22	18	53.9	1
M1-7[a]	68	0.46	−11	25	17.1	
M1-8[a]	43	(0.08)	(+54)	(23)	(2.8)	2
NGC 2346	...	0.90	+9	28	18.6	1, 3
M1-16[a]	83	0.88	+50	25	26.4	
NGC 2440	32	0.10	+44	28	3.6	
VV 47 66 E, 66 S	36	0.22	−55	14	1.5	4
... 66 W, 66 N	78	0.36	...	...	3.2	
NGC 6072	120	1.8	+15	24	28.9	5
M2-9	70	(0.12)	(+79)	(13)	(2.0)	1, 2
NGC 6302	87	0.56	−40	25	19.9	1
NGC 6445	68	0.25	+20	33	11.1	
NGC 6563	130	0.41	−27	32	18.8	
M4-9	72	0.47	−15	17	13.2	6
NGC 6720	48	0.27	−2	22	5.1	7
NGC 7027	260	11.2	+26	23	277.9	1
IRAS 21282+5050[a]	110	2.1	+18	16	40.0	1
IC 5117	57	0.22	−10	16	4.6	
M2-51	110	(0.27)	(0)	(15)	(4.9)	2
NGC 7293	...	1.4	−24	24	7.0	8

[a] Position references. M1-7, M1-8 (Milne 1976); M1-16 (Kwok 1985); IRAS 21282+5050 (de Muizon *et al.* 1986).

NOTES.—(1) Earlier or additional CO observations by others (see text). (2) Tentative detection. (3) Data from Paper 3. (4) VV 47 = PK 164 +31.1, and is often erroneously referred to as NGC 2474-5 (see Barbieri and Sulentic 1977). The CO kinematics are derived from narrow lines at −41 and −69 km s^{-1} at the SE and NW offsets, respectively. (5) Two main spike components at +30 and −1 km s^{-1}. (6) Strong Galactic line on red wing of spectrum. (7) See also Paper 2. (8) Data from Paper 1; V_e from outer ring; T and I representative of outer ring at offsets 405 E, 0 N.

spectra are severely contaminated by Galactic lines. In all cases where the radial velocity of the PN is known (Schneider *et al.* 1983), the actual intensity integrated over the corresponding velocity range is less than the quoted limit. In three cases (Vy 2-2, NGC 7048, and M2-55) it is close to the quoted limit, so there is a very weak hint of emission. Knapp and Morris (1985) have reported a tentative detection of CO(1–0) in Vy 2-2, but from our data we are unable to confirm the presence of CO. NGC 6853 deserves special mention since it shows very extended molecular emission in H_2 (Zuckerman and Gatley 1988). We have searched several positions in CO(2–1) to the level given in Table 1, and many more positions in CO(1–0) to about half this level. Weak CO emission is seen toward the nebula within the expected velocity range. We are, however, unable to unambiguously associate it with the nebula because it is too weak to map and correlate with optical features, and because of the presence of Galactic emission in this direction.

Nineteen PNe in the survey were detected or tentatively detected in CO. The spectra are shown in Figure 1, except for those reported earlier in Papers 1–3. Estimates of the line parameters are listed in Table 2, where the systemic velocity (V_0) is given with respect to the local standard of rest and the expansion velocity (V_e) is taken to be half the full line width at zero intensity. Four of the PNe (NGC 7027, NGC 2346, NGC 6302, and AFGL 618) had previously been detected in CO, as tabulated by Knapp (1987). In addition, during the course of this work, IRAS 21282+5050 was independently detected by Likkel *et al.* (1988) and M2-9 by Bachiller *et al.* (1988).

Three of the detections reported in Table 2 are quite tentative, and the parameters should be viewed with caution. The most doubtful is a marginal feature in M2-9 at $V_0 = 79$ km s^{-1} (see Fig. 1). We include it because Bachiller *et al.* (1988) find a CO(1–0) feature at the same velocity which is sufficiently close to optical radial velocities for M2-9 (e.g. Walsh 1981) that association of the CO with the PN is probable. The CO velocity parameters for the two other tentative detections (M1-8 and M2-51) are consistent, within the large errors, with the optical values listed by Schneider *et al.* (1983) and Sabbadin (1984).

In the other cases where CO is fairly convincingly detected, the line profiles and the velocity parameters suggest association with the PNe, although most have not yet been mapped. For M1-7, M1-16, NGC 6072, and M4-9, V_0(CO) improves considerably upon the very uncertain optical radial velocities listed by Schneider *et al.* (1983). For most objects V_e(CO) is roughly the same as V_e(optical) determined from forbidden lines (e.g., Sabbadin 1984; Sabbadin, Strafella, and Bianchini 1986) but in M1-7, M1-16, and NGC 6563 it is more than twice as large. As far as we know, the CO data for M4-9 provides the first expansion velocity for any species in this object. In the extended PN VV 47, the observations were made at offset positions toward the two symmetric lobes. The CO velocities of these features are in excellent agreement with optical measurements reported by Sabbadin, Strafella, and Bianchini (1986).

Figure 1 and Papers 1–3 show a wide variety of observed CO line profiles in PNe. This is accounted for in part by the angular size of the CO emitting region relative to the beam size. For compact PNe with thick envelopes (e.g., AFGL 618 and M1-16) which are basically unresolved by the beam, the broad profiles are similar to those commonly seen from red giant circumstellar envelopes. For larger PNe comparable in size to the beam, the profiles are still broad but begin to reflect the envelope structure (e.g., NGC 6720). An extreme example of this is the double-spiked spectrum of NGC 2346, and it was shown in Paper 3 that the CO is roughly distributed in the form of a ring; NGC 6072 appears to be somewhat similar. Finally, when the PN is much larger than the beam, individual

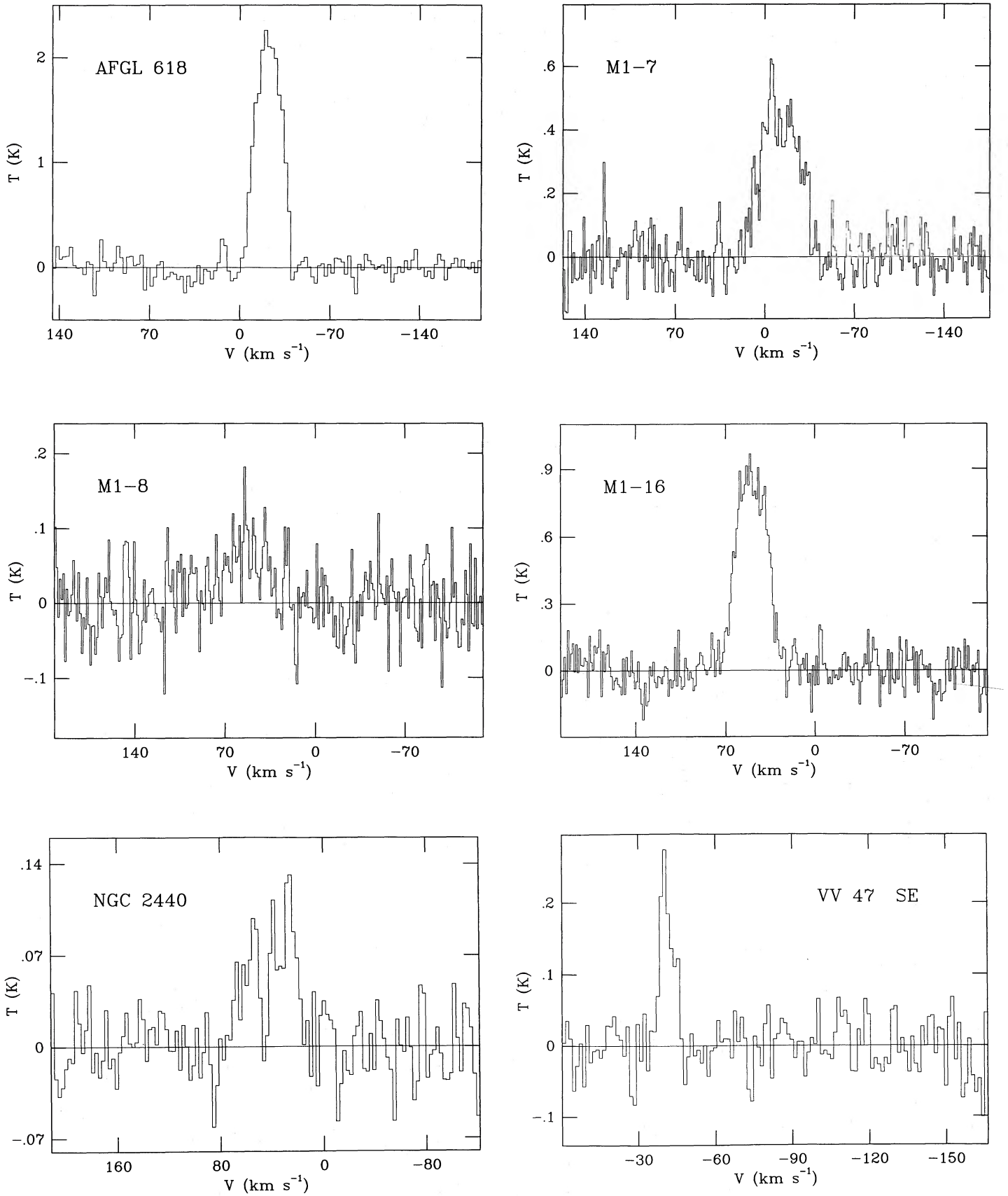

FIG. 1.—Spectra of the survey PNe detected or tentatively detected in CO(2–1). See also Papers 1–3.

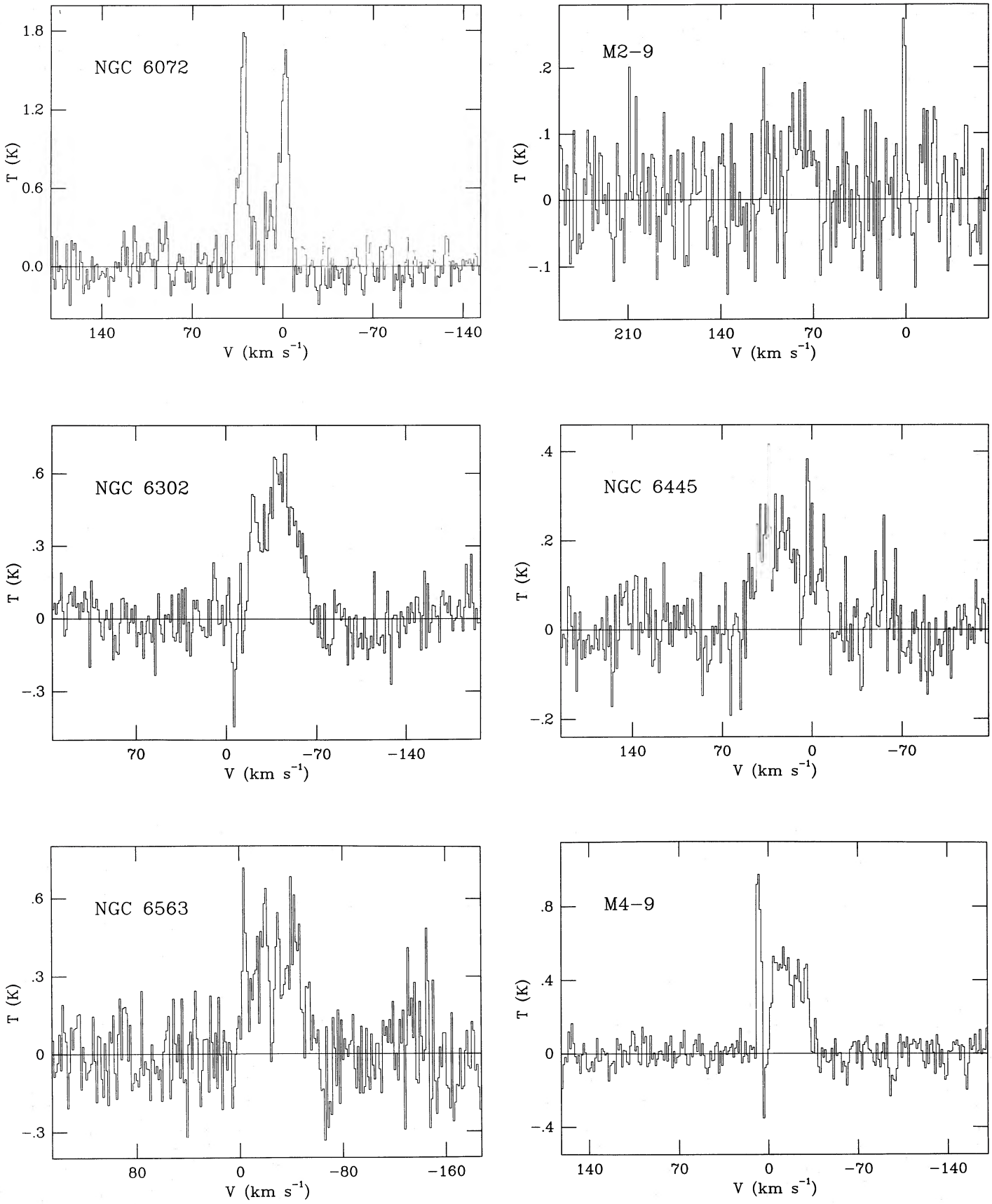

FIG. 1.—*Continued*

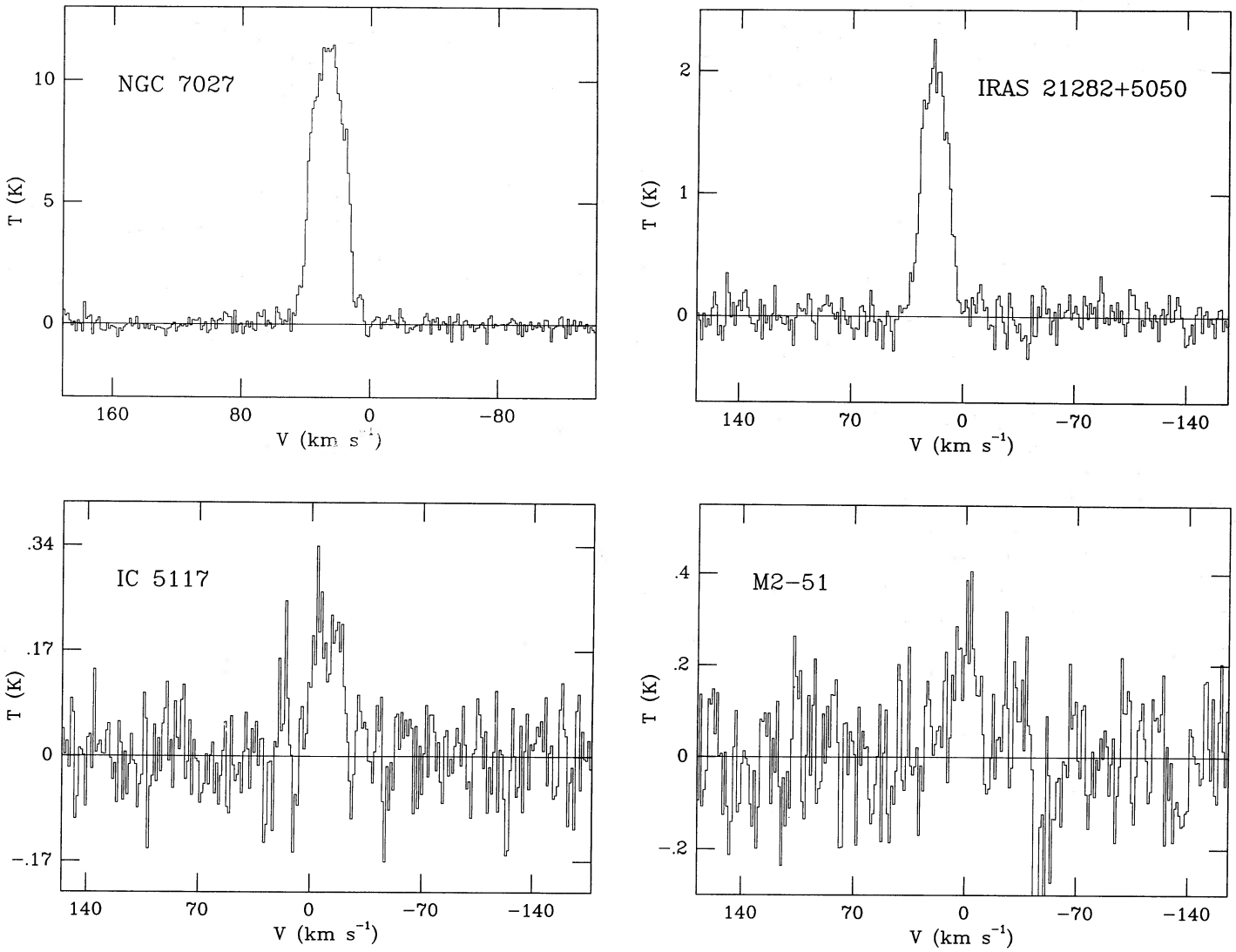

FIG. 1.—*Continued*

molecular condensations may be isolated within the beam and the observed CO profiles can be quite narrow, as in NGC 7293 and VV 47. These cases are of considerable interest for probing the detailed kinematic structure of the molecular gas, as outlined for NGC 7293 in Paper 1.

III. DISCUSSION

a) Characteristics of the Detected Planetary Nebulae

The results of the survey show that observable CO emission is not a rare property of PNe; the few previously known cases are extreme or fairly nearby examples of a more common phenomenon. Although the number of CO detected PNe is still not very large, it does allow some general conclusions on their molecular envelopes to be made. In this section we briefly examine some characteristics of the PNe which show CO emission. In later sections we estimate masses and mass limits for the molecular envelopes and discuss the extent to which evolutionary effects can be studied.

Some relevant properties of the PNe detected in CO are listed in columns (2)–(5) of Table 3. Angular radii are taken from Maciel (1984) and Pottasch (1984) and generally refer to the size of the main optical component of the nebulae. As is well known, the distances to PNe are in most cases poorly determined. Here we adopt in order of preference individual distances given by Gathier (1987) and Sabbadin (1986*a*), and statistical distances from Sabbadin (1986*b*) or means from the catalogs of Acker (1978), Daub (1982), and Maciel (1984). The type I designations are taken from Peimbert and Torres-Peimbert (1983), and the H_2 detections from Zuckerman and Gatley (1988) and Webster *et al.* (1988). B and C morphological types are mainly from Sabbadin (1984, 1986*a*). This classification scheme is a highly simplified description of PNe but does contain some essential features of more detailed classifications. (For example, 63 of the sample PNe with B/C types have also been classified by Zuckerman and Aller [1986]: for 86% of these there is a one-to-one correspondence between B/C type and the presence/absence of BP [bipolar] as the primary description in the more detailed Zuckerman and Aller scheme.) The N/O ratios are mainly from the tabulations of Zuckerman and Aller (1986) and Peimbert and Torres-Peimbert (1983), or from Aller and Czyzak (1983), Aller and Keyes (1987), and Kaler (1983). Special cases are noted in the

TABLE 3

PROPERTIES OF NEBULAE DETECTED IN CO

PN (1)	R (″) (2)	D (kpc) (3)	log (N/O) (4)	Class (5)	M_m ($M_\odot$) (6)	M_i ($M_\odot$) (7)
AFGL 618	0.2	2.0[a]	−0.10	B,[b] I, H_2	2.0(−1)	5.7(−4)
M1-7	4.5	2.5	−0.17	B	7.9(−2)	2.1(−2)
M1-8	11.0	2.8	−0.37	I	1.8(−2)	1.4(−1)
NGC 2346	27.3	0.8	−0.28	B, I, H_2	5.1(−2)	4.4(−2)
M1-16	1.5	5.8	...	...	8.2(−1)	4.7(−2)
NGC 2440	16.2	2.2	+0.18	B, I, H_2	5.6(−2)	6.5(−1)
VV 47	194.0	0.6	+0.08	B, I	1.4(−2)[c]	1.9(−1)[d]
NGC 6072	35.0	1.8	...	B,[b] H_2	5.4(−1)	6.9(−1)
M2-9	8.6	2.8	−0.80	B,[b] H_2	1.3(−2)	1.2(−1)
NGC 6302	22.3	0.7	−0.22	B, I, H_2	1.1(−1)	1.5(−1)
NGC 6445	16.6	2.2	+0.08	B, I, H_2	8.5(−2)	5.6(−1)
NGC 6563	22.6	0.7	+0.25	B	3.3(−2)	2.2(−2)
M4-9	22.1	1.4	...	...	9.1(−2)	1.6(−1)[d]
NGC 6720	35.0	0.7	−0.51	B, H_2	1.0(−2)	8.5(−2)
NGC 7027	5.0	1.1	−0.40	B, H_2	1.7(−1)	7.8(−2)
21282+5050	0.6[e]	2.0[a]	...	...	1.5(−1)	...
IC 5117	0.6	2.1	−0.57	C, H_2	1.5(−2)	4.3(−3)
M2-51	19.6	1.6	−0.43	B	3.6(−2)	1.5(−1)[d]
NGC 7293	330.0	0.1	−0.43	B, H_2	3.9(−3)	4.1(−2)

[a] Nominal distances consistent with the luminosities of compact PNe.

[b] Classified by us as B type on the basis of bipolar structure. For M2-9, the low N/O ratio from Barker (1978) suggests an old population object, but this has been questioned by Calvet and Peimbert (1983). NGC 6072 was classified as non B by Greig (1971), but its CO spectrum and distribution (unpublished), as well as its appearance in the Southern Sky Survey, are similar to NGC 2346: on this basis we reclassify it as B type.

[c] Based on an envelope radius of 93″, the offset at which CO is observed.

[d] Estimated from Balmer line fluxes given by Kaler (1983) and Cahn and Kaler (1971).

[e] Upper limit given by Cohen and Jones (1987).

footnotes to Table 3. A similar compilation of data for the large number of nebulae not detected in CO is used in some of the figures and table entries discussed below.

The detected PNe cover a wide range in angular size and include some very compact objects as well as some of the largest PNe known. Figure 2 shows the distribution of CO intensities with angular radius, and includes for comparison the upper limits of the undetected objects. There is little correlation of the detection rate with angular size. There is also little correlation of the detection rate with distance, in spite of the fact that the envelopes of most PNe are expected to be partially resolved or unresolved by the telescope beam. The detected objects are not simply the nearest: their median distance (1.8 kpc) is similar to that of the whole survey (1.5 kpc). This

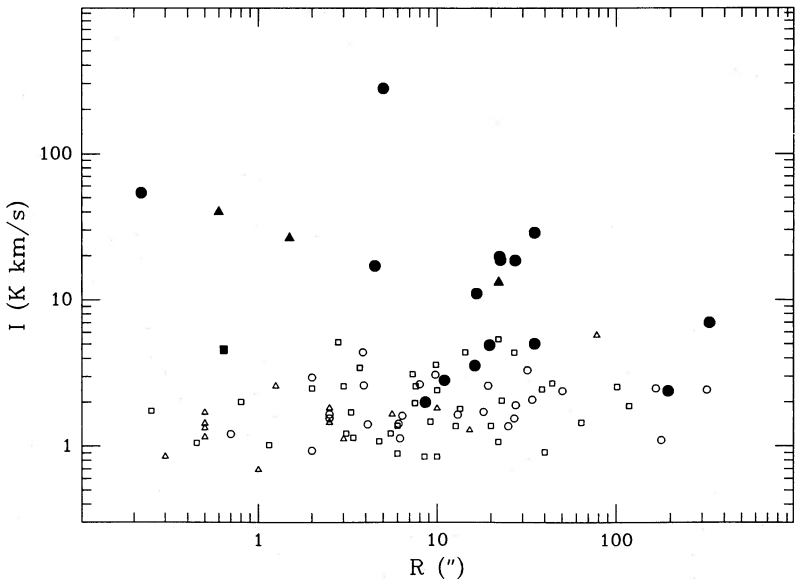

FIG. 2.—Distribution of CO line strength with nebular angular radius. Large filled symbols are detections, or tentative detections; small symbols are upper limits. Circles and squares are young and old population PNe, respectively, according to their morphological type; if this is unknown, the N/O ratio is used instead if available. Triangles are unclassified PNe.

demonstrates that there is a very large range in the CO luminosity of PNe.

These points will be taken up in more detail in later sections. At this stage it is pertinent to ask whether the detected PNe share any common properties. Columns (4) and (5) of Table 3 show that they do: most of them have some form of bipolar structure (type B PNe) and/or have high N/O ratios. Both indicate statistically (e.g., Greig 1972; Kaler 1983; and references therein) that these PNe are younger disk population objects formed from the upper mass range of main-sequence stars which become PNe; for brevity we call them young population PNe. Of the 15 PNe with B/C classifications, 93% are of type B; of the 15 with known N/O ratios, 80% have log (N/O) > -0.5, a subset of which are type I nebulae discussed by Peimbert and Torres-Peimbert (1983).

The significance of this is underscored by considering the CO detection rates for various samples of the survey PNe for which classification data are available, as shown in Table 4. Compared to the survey as a whole, the CO detection rates are higher for types B and I, and PNe with log (N/O) > -0.5, and are lower for type C, and PNe with log (N/O) < -0.5. The detection rate is most strongly related to morphological type, and the probability that the association is real is highly significant (>99.9%). This could be interpreted in terms of the intrinsic properties of the PNe if the different types are similarly distributed with distance, which is roughly the case as indicated by the median distances given in Table 4. To further investigate this point we have also determined the association of morphological type with molecular mass estimates, which effectively correct the CO observations of individual PNe for distance and angular size, as described in the next section. Using the log rank statistic for censored data to deal with the upper limits (Feigelson and Nelson 1985), we find that the association is again highly significant at the level given above. Thus the common characteristics of the detected PNe and the overall statistics of the survey indicate that the PNe with substantial CO envelopes are primarily young population objects.

Infrared H_2 line emission has also been found to be a characteristic of young population PNe. Zuckerman and Gatley (1988) have shown that PNe detected in H_2 are preferentially at low Galactic latitudes. A similar effect is found for CO in the present data but is much weaker than for H_2, probably because we observed few objects at high latitudes. The mean absolute latitudes for the CO detections and nondetections are $7°.2 \pm 1°.8$ and $14°.2 \pm 1°.7$, respectively (where we have excluded NGC 7293 from the averaging because it is much closer than the other PNe). Zuckerman and Gatley (1988) and Webster *et al.* (1988) have also shown that H_2 is associated with bipolar nebulae, which is in accord with the results for CO discussed earlier. It is therefore not surprising to find an association between H_2 and CO detections as shown in Table 4. This comparison is only qualitative since there is a range in threshold and aperture size for the available H_2 data. Nevertheless, the association appears to be highly significant. More extensive H_2 data in the form of maps are needed for a thorough comparative study with CO, which should prove useful in more clearly understanding the physical state of the molecular gas.

TABLE 4

CO Detection Rates for Various Planetary Nebula Samples

Sample	Size	D[a] (kpc)	Detection Rate (%)
Whole survey	95[b]	1.5	20
Type B	36	1.7	39
Type I	20	1.5	35
Log (N/O) > -0.5	40	1.5	30
H_2 detections	18	1.4	61
Type C	36	1.5	3
Log (N/O) < -0.5	30	1.4	10
H_2 nondetections	15	1.0	0

[a] Median distance.

[b] Excluding those for which no limits are given in Table 1.

b) *The Masses of Planetary Nebulae Molecular Envelopes*

A key issue in assessing the role of molecular gas in PNe is the mass of their molecular envelopes, which we estimate here from the CO observations. The estimates involve a number of simplifying assumptions on the physical state and extent of the gas, and unavoidably depend on the adopted distances to the PNe, which were discussed earlier. As a result, the estimates in some cases may be uncertain by an order of magnitude, but the range turns out to be considerably larger.

A basic assumption we make is that the CO(2–1) line emission is optically thin. The velocity integrated emission along a line of sight through a nebula is then proportional to the CO column density in the $J = 2$ level. This is proportional to the total CO column density and the mass column density, if the excitation can be characterized by a single temperature (T_{ex}) and the CO abundance (f) is constant within the molecular gas. We also assume a helium abundance of 0.10. Since the velocity integrated emission (I) measured with the 12 m telescope is the nebular emission integrated over the telescope beam, and the total mass (M_m) is the mass column density summed over the face of the nebula, it is straightforward to show that I (in K km s^{-1}) and M_m (in solar units) are related by the expression: $M_m = 3.0 \times 10^{-7} I D^2 f^{-1} C$, where the distance D is in kpc, and C is a coupling factor which depends on the angular size and geometry of the nebula, and is normalized so that $C = 1$ when the envelope is unresolved by the telescope beam. The numerical factor in the expression depends weakly on T_{ex} over a large range in temperature: the value given is correct for both $T_{ex} = 7$ and 77 K, and deviates by less than a factor of 2 from the correct value over the range $T_{ex} = 5$–170 K, which should bracket most cases of interest. If T_{ex} lies outside this range (e.g., if the PN has an extended molecular envelope of very cool gas) the mass estimate will be a lower limit. The assumption of optically thin emission is likely to be a good approximation in most cases, but again the mass will be underestimated if the emission is optically thick.

In estimating the molecular masses for individual PNe we assume that CO is fully associated and that the O/H and C/H element abundances are the same as in the ionized gas. For the PNe in which both these ratios are reasonably well determined (Zuckerman and Aller 1986) we set f equal to the smaller of the two. For the other PNe, we set f = O/H if O/H is known, or use $f = 3.3 \times 10^{-4}$, which is representative of the previous cases. The O/H ratios are largely taken from the tabulations of Kaler (1980), Aller and Czyzak (1983), and Aller and Keyes (1987). It is important to emphasize that CO may not be fully associated in the bulk of the molecular gas. In addition, the abundance of CO will drop rapidly in regions exposed to the ultraviolet radiation fields of the central star and the interstellar medium (Mamon, Glassgold, and Huggins 1988). In both regions there may be substantial amounts of H_2 but little CO. Since the molecular masses we estimate are associated

with the CO emission, they will in general be lower limits to the total molecular masses.

A final requirement for estimating the masses of extended nebulae is an estimate of the coupling factor C which accounts for the CO emission not sampled by the telescope beam. C depends on both the extent of the emission and the nebular geometry. The only available characteristic size for most PNe is the angular radius (R) of the ionized gas, and we assume that this also characterizes the extent of the CO emission. In two extended PNe where the CO has been partially mapped (Papers 1 and 3), this is roughly the case. We have investigated how various distributions of the molecular gas affect the coupling to the beam, and for simplicity and uniformity we adopt a standard case for all PNe: a thin ring, seen face on, with the beam centered on the rim edge. For this case $C = 0.18R$ for R in arcseconds, when R is much larger than the beam size; $C = 1$ for small R; and intermediate cases are found numerically. This standard configuration applies to few, if any, of the actual observations but it provides a useful estimate for C intermediate between more extreme assumed geometries. For example, for $R = 100''$, values for C obtained for observations centered on face on disks, thin shells, and edge on thin rings, differ from the standard value by factors of 1.5, 2.9, and 0.5, respectively. If the CO distribution is very patchy the appropriate value for C could be very different from the standard. For less extended PNe the coupling uncertainty becomes less, and for PNe small compared to the beam size, $C = 1$, independent of the geometry. Some PNe of small angular size may, however, have very extended molecular envelopes which are larger than the beam, and in these cases the coupling will be underestimated. Clearly our approach is highly simplified, but it should be useful for a first analysis of the observations.

Following the above prescription, values for M_m have been estimated for the detected PNe and the results are listed in Table 3. Upper limits for the nondetections are calculated in the same way and are given in Table 1. The distribution of M_m with distance is shown in Figure 3, where the symbols for nebular types are the same as in Figure 2. The absence of data points in the lower right of Figure 3 reflects the sensitivity limit of the survey data; the scatter in the upper limits for a given distance is introduced by the different noise levels in the spectra, CO abundance estimates, and angular sizes of the individual PNe.

In spite of the considerable uncertainties in estimating M_m from the observations there is clearly a very large range. As expected, the detected PNe are for the most part those with the highest values of M_m at a given distance. For these PNe, M_m is much larger than the typical mass (10^{-3}–10^{-4} $M_\odot$) associated with vibrationally excited H_2 emission, which is usually interpreted as shocked gas (e.g., Isaacman 1984*b*; Zuckerman and Gatley 1988). The highest values of M_m lie in the range 0.1–1.0 $M_\odot$, but the true values of M_m could be somewhat larger because of our conservative assumptions. To give some idea of the uncertainties involved, we note that Bachiller *et al.* (1988, 1989) have estimated the molecular masses for NGC 2346 and AFGL 618 using different assumptions than used here, and obtain results that are larger by factors of 5–12 (for the same adopted distances). Thus the upper mass range of molecular envelopes is comparable to or larger than the ionized masses of fully developed PNe, which strongly supports the idea that at least some PNe form by the ionization of a molecular envelope.

Figure 3 also shows the difference between the young and old population PNe, which was discussed earlier. The upper

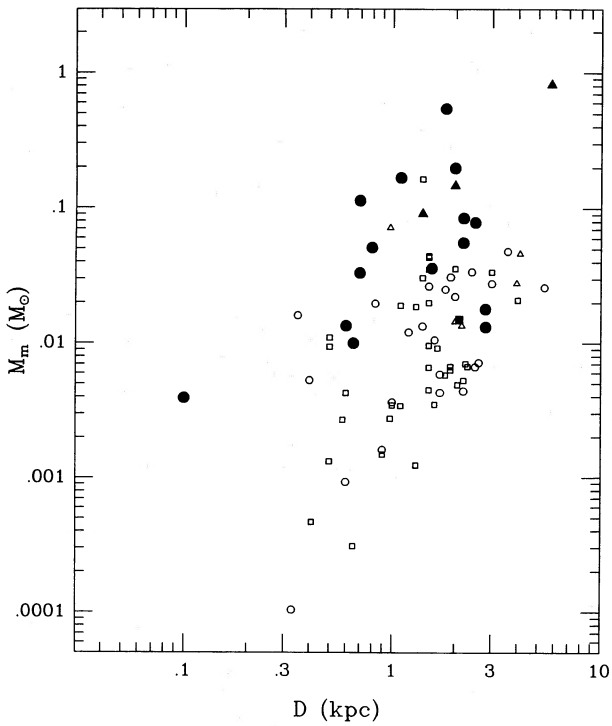

FIG. 3.—Distribution of molecular mass estimates with nebular distance. Symbols are the same as in Fig. 2.

envelope of the mass distribution with distance consists primarily of detected, young population objects. Few, if any, old population PNe have envelopes with $M_m > 5 \times 10^{-2}$ $M_\odot$, and the majority of the upper limits for this class are considerably lower. There is also a rough correlation of envelope mass with the location of the central stars on the H-R diagram, which is expected because the population indicators used here do the same. Eight out of nine PNe detected in CO which are plotted in the H-R diagram by Pottasch (1984) have very high effective temperatures and lie along evolutionary tracks for core masses of greater than 0.6 $M_\odot$. However, we do not pursue the issue here in any detail because of the large uncertainties which affect the H-R diagram for PNe.

The presence of molecular gas in PNe indicates that they are ionization bounded, at least in some directions, and this issue has been discussed for individual nebulae in connection with H_2 by Zuckerman and Gatley (1988). Since our results and those for H_2 show that the presence of molecular gas is to some extent a population effect, they might suggest a difference in the opacity in the Lyman continuum between the different populations of PNe. From a study based on Zanstra temperatures, Sabbadin (1986*b*) does indeed find that B nebulae are largely optically thick throughout most of their evolution, whereas C nebulae are optically thin, except in the earliest, compact stages. This is broadly consistent with the molecular line results.

It is interesting to note that the one PN detected in CO which is probably an older population object (IC 5117) is compact and its molecular mass is about an order of magnitude lower than the most massive envelopes. A number of other fairly small PNe also have low limits on the mass of their molecular envelopes. This suggests that in addition to the different luminosity evolution of high- and low-mass central stars which will affect the molecular properties of PNe (Zuckerman

and Gatley 1988, and references therein), the initial mass or mass-loss rate of the progenitor envelopes may also depend on population type. The bipolar structure of the envelopes also probably plays a role. Envelopes with rings or similar structure will produce higher local densities than more uniform distributions for a given mass and will more effectively shield the molecular gas from dissociating radiation.

c) *Nebular Evolution*

We have shown that an extreme class of young population PNe have substantial masses of molecular gas which may be comparable to or exceed the typical ionized masses of fully developed PNe. In addition, in two of these objects which are extended (NGC 2346 and NGC 7392), mapping shows that the CO emitting gas is closely associated with the ionization fronts of the nebulae (Papers 1 and 3). It is difficult to avoid the conclusion that these nebulae grow by the ionization of previously ejected molecular gas. To investigate this further we first confine our attention to the PNe detected in CO, excluding the tentative cases and the older population PN IC 5117. Since there is a large range in the properties of PNe, we hope thereby to isolate a set of roughly similar, extreme objects.

For these PNe, Figure 4 shows the distribution of M_m with nebular radius, which is calculated from the adopted distances and angular sizes listed in Table 3. This figure should be viewed with some caution as it depends in both coordinates on the adopted distances and is affected by other systematic uncertainties in M_m discussed earlier. In particular, all the PNe with radii less than 0.06 pc show somewhat rounded CO line profiles which suggests that the emission is optically thick. In addition, these PNe probably have extended envelopes of cool CO which are not well accounted for in our treatment of the molecular excitation and the telescope coupling. Both these effects will increase M_m for the smaller PNe. Thus the weak trend of decreasing M_m with increasing radius in Figure 4 is probably, in fact, somewhat stronger. Even the larger PNe, however, are able to retain a substantial amount of their initial molecular envelopes.

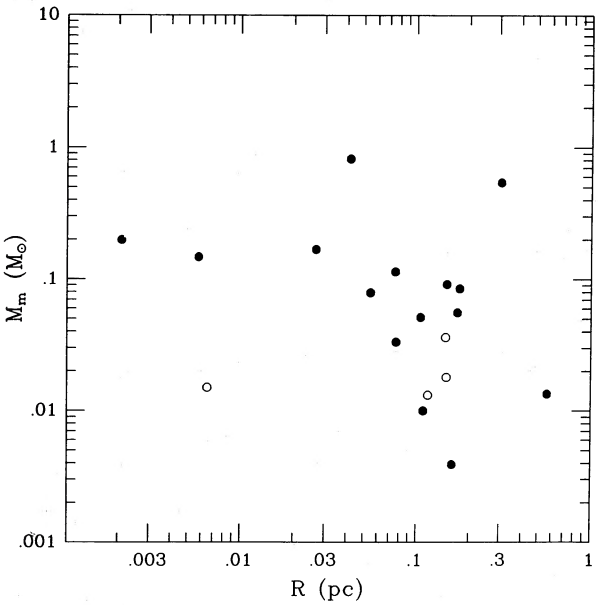

FIG. 4.—Distribution of molecular mass with nebular radius for the CO detected PNe. Open circles are tentative detections and the compact object IC 5117, which is probably from the older population (see text).

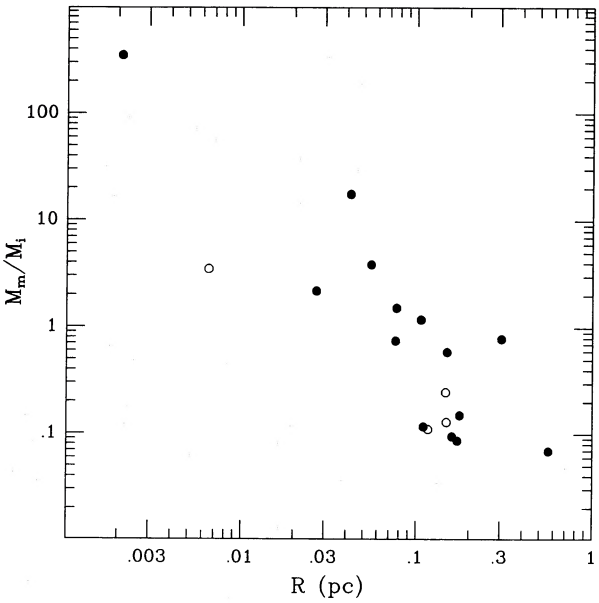

FIG. 5.—Distribution of the molecular/ionized mass ratio with nebular radius for the CO detected PNe. Symbols are the same as in Fig. 4. IRAS 21282+5050 is not included as the ionized mass is very uncertain.

The relation of M_m to the mass of ionized gas (M_i) is shown in Figure 5, which plots the ratio M_m/M_i against nebular radius. The values used for M_i are given in Table 3. They are mainly taken from Gathier (1987) or calculated in a similar way using available 5 GHz radio continuum observations. For five of the PNe the adopted distances are statistical, so M_i and the distance are not independent. However, the distance largely cancels in forming the mass ratios.

Figure 5 shows a large systematic decrease in M_m/M_i with increasing radius which is consistent with the idea that the nebulae form by the ionization of their molecular envelopes from within by the central star. The observed effect is largely due to an increase in M_i with radius. This is well known for other samples of PNe (e.g., Pottasch 1980) and is usually interpreted as indicating an unseen reservoir of neutral gas which becomes ionized as the nebulae expand. Since all the PNe in the present sample have substantial molecular envelopes, there is ample material for the growth of the ionized nebulae. H I has been searched for in several of them and detected in one, NGC 6302 (Rodriguez and Moran 1982), where the mass in H I is somewhat less than M_m. The mass of ionized plus molecular gas in these PNe is typically 0.2 $M_\odot$, and it shows no correlation with radius, as might be expected if it forms a major part of the mass budget. The total masses, however, are likely to be somewhat larger because of our conservative estimates of M_m, as well as the neglect of atomic gas, and H_2 regions where the CO is largely photodissociated.

Figure 5 shows that the radius at which the dominant observed mass component changes from CO bearing molecular gas to ionized gas is about 0.1 pc. The largest PNe in which CO is detected have M_m/M_i of about 0.1, so these nebulae still retain a moderate fraction of their initial molecular envelopes, which is consistent with the limited range of M_m shown in Figure 4. These properties are consistent with the formation of the PNe from red giant envelopes with large mass-loss rates.

Mamon, Glassgold, and Huggins (1988) have shown how the extent of the CO envelopes will be limited by CO photodissociation by the interstellar radiation field. Using their standard parameters, the radius at which CO is reduced to half its initial value (and it falls rapidly thereafter) is 0.3, 0.08, and 0.02 pc for mass-loss rates of 10^{-4}, 10^{-5}, and 10^{-6} $M_\odot$ yr^{-1}, respectively. The corresponding values of M_m (as defined previously) are 2, 5×10^{-2}, and 1×10^{-3} $M_\odot$, respectively. (The total mass including molecular gas where CO is dissociated may, of course, be larger depending on the duration of mass loss.) When the mass loss ceases, M_m will decrease due to the expansion of the inner radius of the envelope and the onset of ionization. When the size of the photodissociation region of the central star exceeds the characteristic size of the CO envelope, the bulk of the CO will be destroyed. Clearly the properties of the CO detected PNe are consistent only with the highest mass-loss rates. More detailed comparisons, however, would need to take into account the complex structure of the envelopes. All the PNe in the present sample are bipolar in some way, and in two cases where the CO has been mapped, it is roughly in the form of dense rings (Papers 1 and 3). These structures will play an important role shielding the molecular gas from both external and internal radiation.

It is important to emphasize that the above results relate only to the extreme class of young population PNe detected in CO. As will be clear from Figure 3, there is a large range in the upper limits for nondetected PNe, which is due in part to the range in angular sizes and distances. If we focus on the 40 PNe with small radii (<0.1 pc) which are likely to retain more of their initial CO envelopes, the typical (median) limit on M_m is 5×10^{-3} $M_\odot$. The limits on M_m/M_i are also lower than for the CO detected PNe and fall below the relation of Figure 5 by a mean factor of 20. Sixty-five percent of these PNe are C types, and the one detected member of this class, IC 5117, is compact (0.007 pc), with $M_m/M_i = 3$. There is clearly a large range in the CO properties of PNe: many, particularly the older population PNe, have low CO molecular masses and this gas is not the main mass component of the nebulae for most of their evolution. In the light of our earlier discussion, the variations among PNe can probably be accounted for by the different luminosity evolution of the central stars and a modest range in mass-loss rates; variations in the CO shielding due to different envelope structures are also likely to play a role. A deep CO search of compact PNe would be of interest to more clearly define the CO mass function of the progenitor envelopes.

IV. CONCLUSIONS

The results of this survey show that millimeter CO emission is a useful probe of molecular gas in PNe. Several new detections are reported, and together with earlier results allow some general conclusions to be made on the importance of this component of the nebulae.

First, the observations provide rough estimates or limits on the mass of molecular gas in PNe, which ranges from about 1 $M_\odot$ to less than 10^{-3} $M_\odot$; for reasons given in the text, these estimates tend to be on the low side, especially for compact PNe. Second, substantial CO envelopes are primarily a property of young population PNe. Third, these results also provide a preliminary description of the role of the molecular gas in the evolution of the nebulae. For the extreme class of young population PNe detected in CO, the mass ratio of molecular to ionized gas decreases with increasing radius, as expected if the nebulae grow as the molecular envelopes become ionized. The molecular gas in these PNe is the dominant observed mass component, at least until the nebulae grow to radii larger than about 0.1 pc, where the bulk of the CO will be dissociated. In other PNe, particularly the older population, CO emission is less evident. In addition to the slower luminosity evolution of low-mass central stars, lower mass-loss rates, less effective CO shielding, or both may account for this. More sensitive searches as well as detailed studies of individual PNe in CO and other neutral species will help develop a more quantitative picture.

We thank B. Zuckerman for helpful comments. This work was supported in part by grant AST 86-16646 from the National Science Foundation.

REFERENCES

Acker, A. 1978, *Astr. Ap. Suppl.*, **33**, 367.
Acker, A., Gleizes, F., Chopinet, M., Marcout, J., Ochsenbein, F., and Roques, J. M. 1982, *Catalog of the Central Stars of True and Possible Planetary Nebulae* (*Pub. Spec. C. D. S.*, No. 3).
Aller, L. H., and Czyzak, S. J. 1983, *Ap. J. Suppl.*, **51**, 211.
Aller, L. H., and Keyes, C. D. 1987, *Ap. J. Suppl.*, **65**, 405.
Bachiller, R., Gomez-Gonzalez, J., Bujarrabal, V., and Martin-Pintado, J. 1988, *Astr. Ap.*, **196**, L5.
Bachiller, R., Planesas, P., Martin-Pintado, J., Bujarrabal, V., and Tafalla, M. 1989, *Astr. Ap.*, in press.
Barbieri, C., and Sulentic, J. W. 1977, *Pub. A.S.P.*, **89**, 261.
Barker, T. 1978, *Ap. J.*, **220**, 193.
Cahn, J. H., and Kaler, J. B. 1971, *Ap. J. Suppl.*, **22**, 319.
Calvet, N., and Peimbert, M. 1983, *Rev. Mex. Astr. Ap.*, **5**, 319.
Cohen, M., and Jones, B. F. 1987, *Ap. J.* (*Letters*), **321**, L151.
Daub, C. T. 1982, *Ap. J.*, **260**, 612.
De Muizon, M., Geballe, T. R., d'Hendecourt, L. B., and Baas, F. 1986, *Ap. J.* (*Letters*), **306**, L108.
Feigelson, E. D., and Nelson, P. I. 1985, *Ap. J.*, **293**, 192.
Gathier, R. 1987, *Astr. Ap. Suppl.*, **71**, 245.
Greig, W. E. 1971, *Astr. Ap.*, **10**, 161.
———. 1972, *Astr. Ap.*, **18**, 70.
Healy, A. P., and Huggins, P. J. 1988, *A.J.*, **95**, 866 (Paper 3).
Higgs, L. A. 1969, *J.R.S. Canada*, **63**, 200.
Huggins, P. J., and Healy, A. P. 1986*a*, *Ap. J.* (*Letters*), **305**, L29 (Paper 1).
———. 1986*b*, *M.N.R.A.S.*, **220**, 33P (Paper 2).
Isaacman, R. 1984*a*, *M.N.R.A.S.*, **208**, 399.
———. 1984*b*, *Astr. Ap.*, **130**, 151.
Kaler, J. B. 1980, *Ap. J.*, **239**, 78.
Kaler, J. B. 1983, *Ap. J.*, **271**, 188.
Knapp, G. R. 1987, in *Late Stages of Stellar Evolution*, ed. S. Kwok and S. R. Pottasch (Dordrecht: Reidel), p. 103.
Knapp, G. R., and Morris, M. 1985, *Ap. J.*, **292**, 640.
Kwok, S. 1985, *A.J.*, **90**, 49.
Likkel, L., Forveille, T., Omont, A., and Morris, M. 1988, *Astr. Ap.*, **198**, L1.
Maciel, W. J. 1984, *Astr. Ap. Suppl.*, **55**, 253.
Mamon, G., Glassgold, A. E., and Huggins, P. J. 1988, *Ap. J.*, **328**, 797.
Milne, D. K. 1973, *A.J.*, **78**, 239.
———. 1976, *A.J.*, **81**, 753.
Mufson, S. L., Lyon, J., and Marionni, P. A. 1975, *Ap. J.* (*Letters*), **201**, L85.
Payne, H. E., Phillips, J. A., and Terzian, Y. 1988, *Ap. J.*, **326**, 368.
Peimbert, M., and Torres-Peimbert, S. 1983, in *Planetary Nebulae*, ed. D. R. Flower (Dordrecht: Reidel), p. 233.
Pottasch, S. R. 1980, *Astr. Ap.*, **89**, 336.
———. 1984, *Planetary Nebulae* (Dordrecht: Reidel).
Rodriguez, L. F., and Moran, J. M. 1982, *Nature*, **299**, 323.
Sabbadin, F. 1984, *Astr. Ap. Suppl.*, **58**, 273.
———. 1986*a*, *Astr. Ap. Suppl.*, **64**, 579.
———. 1986*b*, *Astr. Ap.*, **160**, 31.
Sabbadin, F., Strafella, F., and Bianchini, A. 1986, *Astr. Ap. Suppl.*, **65**, 259.
Schneider, S. E., Terzian, Y., Purgathofer, A., and Perinotto, M. 1983, *Ap. J. Suppl.*, **52**, 399.
Walsh, J. R. 1981, *M.N.R.A.S.*, **194**, 903.
Webster, B. L., Payne, P. W., Storey, J. W. V., and Dopita, M. A. 1988, *M.N.R.A.S.*, **235**, 533.
Zuckerman, B., and Aller, L. H. 1986, *Ap. J.*, **301**, 772.
Zuzkerman, B., and Gatley, I. 1988, *Ap. J.*, **324**, 501.

A. P. HEALY and P. J. HUGGINS: Department of Physics, New York University, 4 Washington Place, New York, NY 10003